Supplementary information for “Growth and electronic properties of bi- and trilayer graphene on Ir(111)”

**Claus F. P. Kastorp, David A. Duncan, Martha Scheffler, John D. Thrower,
Anders L. Jørgensen, Hadeel Hussain, Tien-Lin Lee, Liv Hornekær, and
Richard Balog**

Determination of the number of graphene layers from STM:

The number of graphene layers in different areas can be determined by investigating the different moiré patterns and the height of the steps between different islands. Figure S1a shows the same image as Figure 2a in the main article, but with three different squared regions of interest marked. The colors of the squares correspond to the colors of the frames in Figure S1b-d, which show magnifications of the different areas that make it possible to distinguish the moiré pattern in each region.

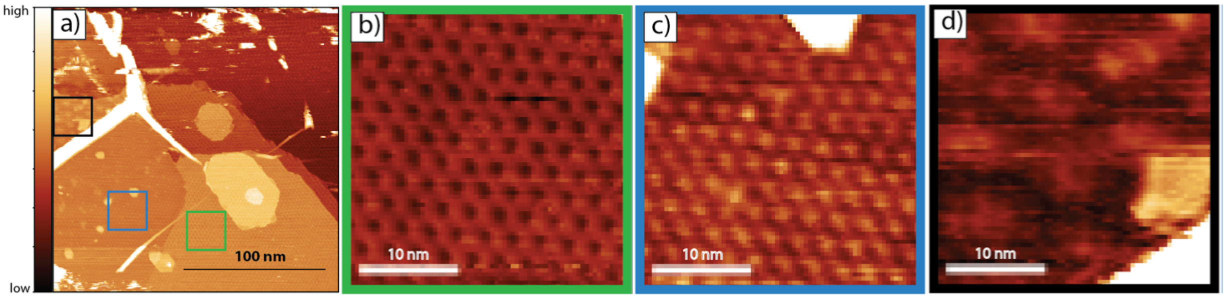

Figure S1: *Enhancements of the various Moiré patterns found on the surface.* ***a)*** *The STM image from the same area as in Figure 1a in the main article with color-coded regions of interest. The colors of the frames in* ***b), c),*** *and* ***d)*** *correspond to the colored regions of interest to indicate the position of each cutout. All selected regions show a characteristic moiré structure with 25Å periodicity. However in* ***d)*** *an additional superposed pattern with a larger periodicity (75 Å) is observed and ascribed to two layers of graphene with a relative rotation.*

In Figures S1b and S1c, patterns can be seen that have the characteristic shape and periodicity of well aligned monolayer graphene on Ir(111) [1,2]. The pattern in Figure S1c has the same orientation and periodicity as in S1b, but has an inverted perceived structure. This is not simply a matter of contrast, since both patterns are consistently scanned during the same lines over a large portion of the image. The pattern in Fig S1c is ascribed to bilayer graphene where both sheets are aligned with each other and with the substrate. This can be shown from the following analysis:

In Figure S1d, two patterns are present: one which is similar to the pattern in Figure S1c and a pattern with a larger periodicity. The larger one has a hexagonal symmetry, with a periodicity of 75 Å and has a rotation of 30 +/- 1 degrees from the pattern in Figure S1c. By applying the analysis outlined in Latychevskaia *et. al*. [3], the 75 Å periodicity of this pattern can be achieved by rotating the two sheets ca. 1.88°. This in turn produces a moiré pattern, which is rotated by 89 degrees with respect to the original structure. When six-fold symmetry is considered, this is equivalent to an angle of 29 or 31 degrees, which is consistent with the measured angle between the two structures depicted in Figures S1c and S1d.

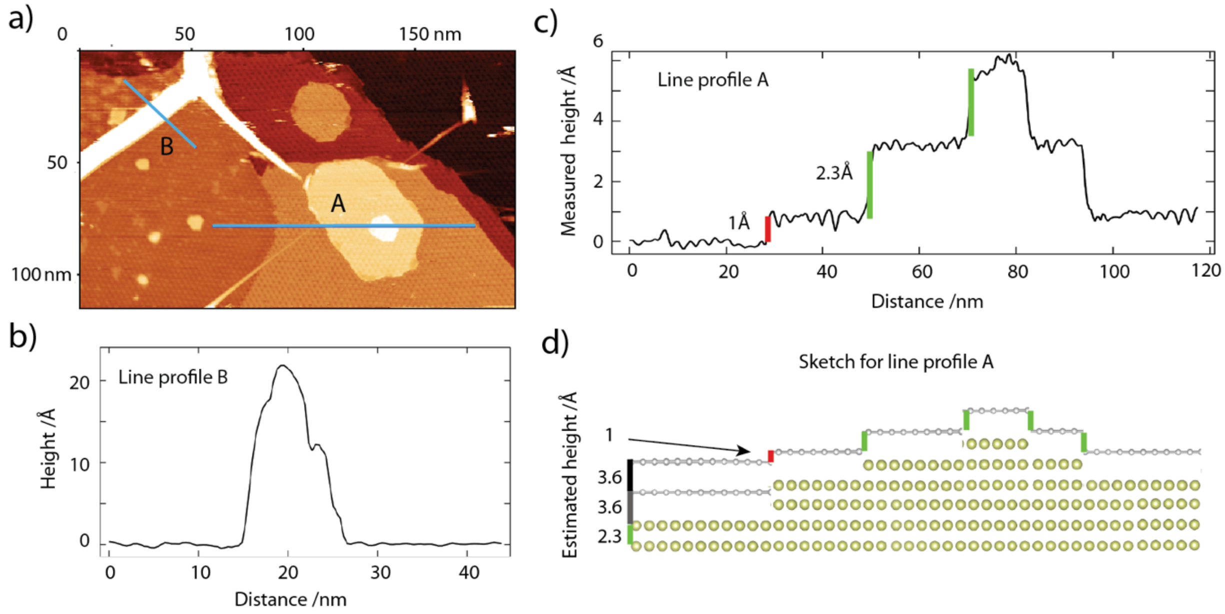

Figure S2: *Coverage analysis based on step heights.* ***a)*** *Section of Figure S1a with line profiles indicated.* ***b)*** *The upper left line profile with a ridge separating two domains which have the same apparent height* ***c)*** *The line profile A with step heights indicated. From left to right, the line crosses a 1 Å step and then has a series of steps of 2.3 Å high.* ***d)*** *Sketch of the possible structure underlying the line profile A. The perceived step heights are 2.3 Å for iridium step and 3.6 Å for spacing between graphene layers.*

The number of layers in the rest of the figure can be determined by analyzing the measured heights of various steps across islands, noting that the expected spacing between two Ir(111) sheets is ca. 2.2 Å and the spacing between either two graphene layers or a graphene layer and the Ir(111) surface is ca. 3.4 Å.

By comparing the height difference between the rotated and non-rotated areas on the opposite side of the wrinkle, the line profile B in Figure S2b, we find that these areas are at the same height. We therefore ascribe these two areas to represent bilayer graphene.

Figure S2c shows the line profile A as indicated in Figure S2a. Most steps have an apparent size of 2.3 - 2.4 Å, which represent the Ir(111) step height with an uncertainty in the calibration of up to 10 % in the direction out of the plane. On the border between the two areas with the same but inverted moiré (as shown in S1b and S1c), a height difference of about 0.9 - 1.0 Å is found. This value can be obtained by assuming two graphene layers on the left hand side of the step (as obtained from analysis above), and a single graphene sheet on top of two additional iridium layers. Figure S2d shows a sketch of the situation. Continuing along the line profile from left to right we find a step height of 2.4 Å Therefore the small islands seen in the right half of Figure S2a are due to Iridium.

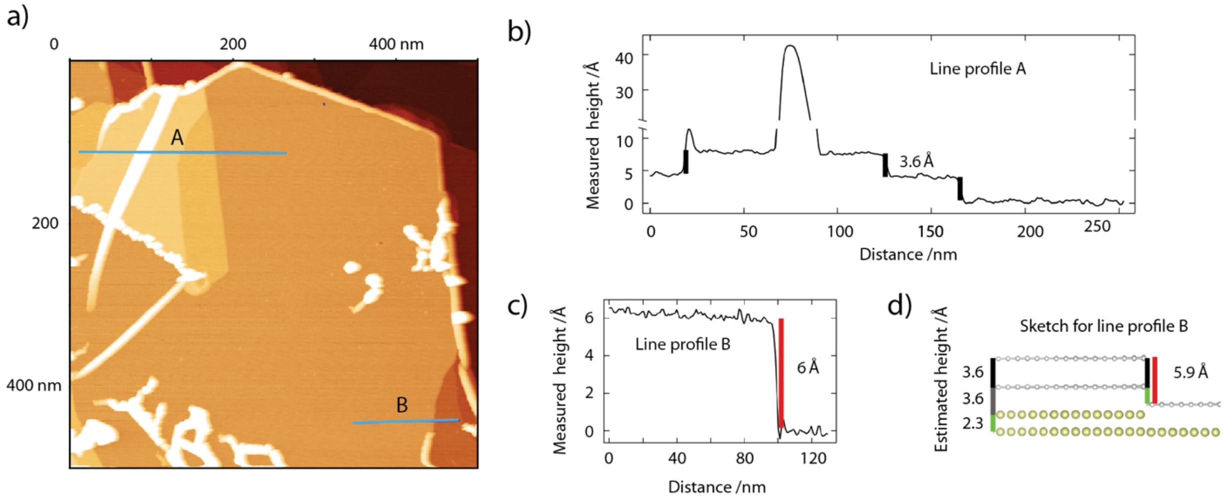

Figure S3: *Coverage analysis for Figure 2b based on step heights.* ***a)*** *A cutout of figure 2b with line scans indicated.* ***b)*** *The upper left line profile from a) (top left) with step heights written. The line crosses several graphene steps, which indicate a multilayer island, and a tall ridge, which is a wrinkle in the top sheet.* ***c)*** *The lower right line profile from a). It shows a single step of 6 Å, which would correspond to going across a graphene step and an iridium step simultaneously.* ***d)*** *Sketch of the structure underlying the line scan in c) under the assumptions described in the text. It shows Ir layers (yellow), graphene layers (grey), and their perceived height differences. The total perceived height of the step is indicated and matches well with the observed line profile in c).*

In Figure S3 the superstructure is not resolved, and therefore the analysis is based solely on the step heights. Figure S3a (same as Figure 2b in the main article) shows the STM image with two relevant line profiles indicated. Line profile A, shown in Figure S3b, has several steps of 3.6 Å and a ridge, where the height level is the same on both sides. This ridge is ascribed to a wrinkle in the top graphene layer, while the 3.6 Å match the graphene step height including the 10 % calibration uncertainty as found for iridium step heights.

Taking the line profile in the bottom of the image, Figure S3c, we find a step height of 6 Å, which would correspond to an Ir(111) step plus a graphene step, see the sketch in Figure S3d. Since XPS and ARPES (Figures 1, 3, and 4 in the main article) indicate large amounts of bilayer graphene, this step is assumed to be a step between monolayer and bilayer. Taking this result into account, the large central area represents bilayer graphene, while the island in the top-left part of the image (profile A) has three and four layers on the both sides of the wrinkle.

Structural parameters and partial bilayer graphene coverage:

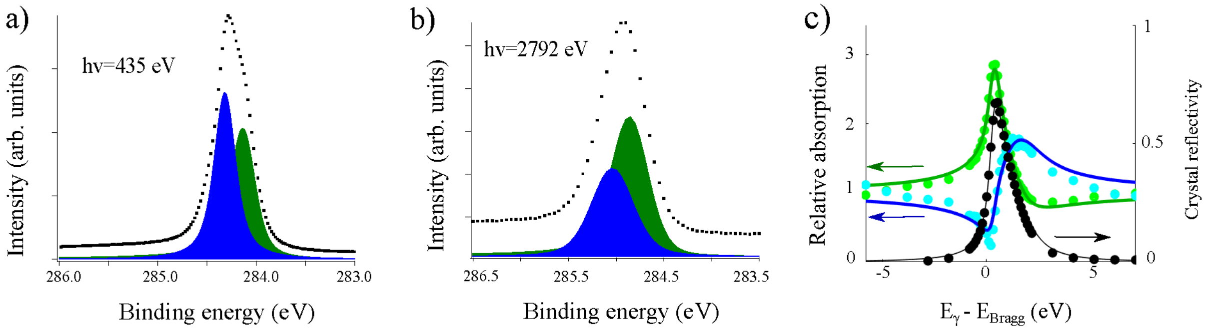

Figure S4: *C1s Photoemission spectra taken at an estimated 1.6ML coverage.* ***a)*** *spectrum taken at E_γ = 435 eV. Two peak components can be resolved (blue and green). The higher binding component (blue) is associated with overlayer graphene and is positioned at 284.13 eV. The peak at lower binding energy (green) represents graphene in contact with the Ir(111) surface, and is located at 284.32 eV.* ***b)*** *Spectrum aquired at the same sample as in a, but at a photon energy of E_γ = 2 792 eV. Again, two components can be resolved, but the ratio between the two peaks has changed due to a lower attenuatin at high kinetic energies.* ***c)*** *Relative absorption for the top layer (light blue data, dark blue fit) and bottom layer peaks (light green data, dark green fit) with the crystal reflectivity (black data points and fit) as the photon energy is scanned through the Bragg condition. Arrows indicate appropriate axes.*

Figure S4 shows photoemission spectra for an intermediate coverage between one and two layers of graphene on average (using a similar analysis as described in [4]). The soft x-ray spectrum in Figure S4a, indicates a sample which has about 65% of area covered with bilayer graphene. The hard x-ray spectrum in Figure S4b indicates a coverage of 60% for the second layer. These two estimates correspond well to each other.

The XSW rocking curves shown in Figure S4c give parameters of F^H = 0.66 and P^H = 0.53 for the lower layer (green), which would correspond to a mean position of d = 3.40 Å above the Ir(111) surface. For the upper layer (blue), these values are F^H = 0.81 and P^H = 0.06, corresponding to d = 6.79 Å. The positions of single and bilayer graphene are in agreement with those found for higher coverage, shown in Figure 3 in the main article. The coherent fractions are, however, much better for this lower coverage bilayer graphene. This is an indication of less stress in both layers as compared to a higher coverage scenario.

Replica bands in the hydrogenated system

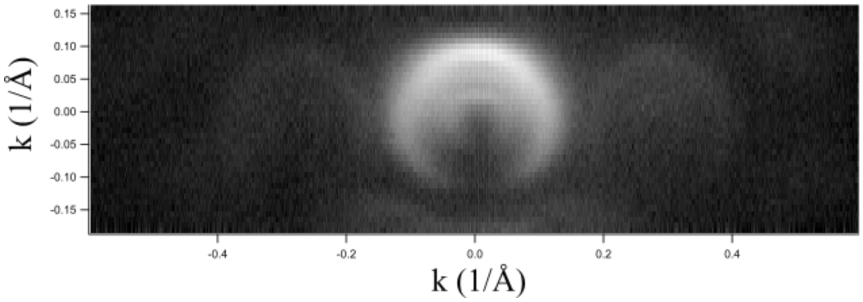

Figure S5: *A constant energy map of the H-functionalized multilayer graphene at a binding energy of 0.4 eV and with photon energy of* E_γ *= 105 eV. In the main part of the band structure, circles associated with the three separate bands can be identified. In the replica cones on either side, only the outermost and innermost bands can be clearly resolved.*

Figure S5 shows a constant energy map from the ARPES measurement taken of the multilayer graphene sample after functionalization with vibrationally excited H_2. In the main structure, three separate circles can be outlined, which correspond to the three bands described in the main text. The outermost and innermost circles, which are ascribed mainly to bilayer areas, can be traced in the replica bands. This is interpreted as large prevalent domains of bilayer graphene modulated by the moiré potential in agreement with the conclusion driven from the non-hydrogenated samples. The middle cone, which comes from trilayer islands, is not resolved in the replica bands. This could be caused either by the complete absence of a replica band, or simply the result of the intensity of the trilayer signal being too low.

Determination of monolayer coverage from XPS and XSW of hydrogenated bilayer:

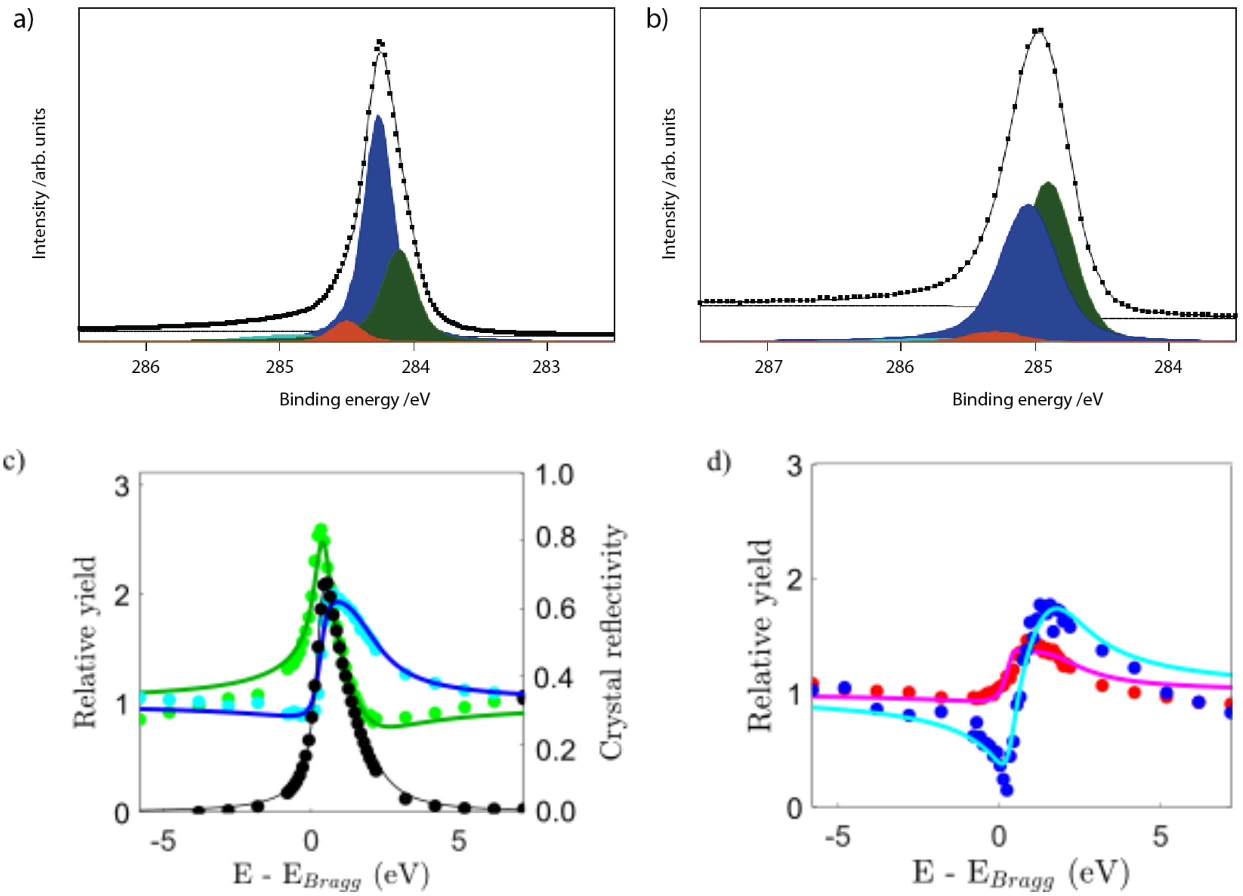

Figure S6: *XPS results from the hydrogenated BL graphene.* ***a)*** *Spectrum acquired at* $E_\gamma = 435$ *eV. The monolayer component (green color) drops in intensity, while two new components appear. These are ascribed to* sp^3 *in the monolayer regions (red color) and most likely hydrogenated defects (cyan color). When attenuation is taken into account, the amount of hydrogenation suggests presence of ca. 15 % monolayer graphene area on the surface.* ***b)*** *Spectrum acquired at* $E_\gamma = 2\ 792$ *eV. The same components can be identified as in a).* ***c)*** *Relative adsorption with varying photon energy close to the Bragg energy for* sp^2*-carbon in the interface layer (light green data points, dark green fit) and higher layer(s) (light blue data, dark blue fit). The reflectivity is shown in black.* ***d)*** *Relative adsorption for* sp^3*-carbon in the monolayer area (dark red data, light red fit) and the* sp^3*-comonent in the upper layers (dark blue data, light blue fit).*

In order to determine the amount of uncovered monolayer graphene on the surface, the hydrogenated sample is investigated with XPS. The spectrum acquired at a photon energy of $E_\gamma = 435$ eV can be seen in Figure S6a. When compared to Figure 1a of the main article, the monolayer component falls in intensity as expected, while two new components appear at higher binding energies: one at an energy expected for sp3 carbon in graphene on Ir(111) [5], and one at even higher binding energies which is ascribed to functionalisation of defects and the like in the top layer. When taking into acount that approx 40% of the exposed monolayer graphene can be functionalized with vibrationally excited molecular hydrogen [5] and the fact that the signal of the exposed graphene is not attenuated, the amount of area covered with bare monolayer graphene is estimated to be ca. 15 % of the surface.

The same components are also observed in Figure S6b, where a photon energy of E_γ = 2 792 eV is used. When the lower attenuation of the photoelectrons at this energy is taken into account, the amount of bare monolayer is 15 % or slightly less, although this number comes with a significant uncertainty due to the low intensity of the sp^3 component. The relative intensities of the top layer components and the interface layer components are consistent with the ones observed for the clean sample in Figure 3 of the main article.

In Figure S6c and S6d, the relative absorption curves in an XSW for each of the four components are shown. Relatively large overlap between the first three peaks at lower BE site imposes large uncertainity to the obtained values. All extracted structural parameters can be seen in table S1. The coherent positions for sp2 components are lower than for the non-hydrogenated system. For monolayer component this is partly due to the hydrogen functionalization as seen in [6]. For bilayer component the large overlap with the sp3 component may be responsible for the reduction of the coherent fraction. Despite all the uncertainities, the estimnated coherent positions of the sp^2-components are close to those seen in the non-hydrogenated system, whereas the lower BE sp^3-component is close to the position of the sp^3-hybridised carbon in hydrogentaed monolayer graphene [6], noting that coherent positions of 0 and 1 are equivalent.

Table S1: Structural parameters found by XSW on the hydrogenated sample.

Component	$\mathbf{F^{111}}$	$\mathbf{P^{111}}$	**Av. Distance from the substrate**
Lowest layer sp^2	0.56	0.58 ± 0.03	3.51 ± 0.07 Å
Higher layer sp^2	0.43	0.15 ± 0.03	6.99 ± 0.07 Å
Monolayer sp^3	0.30	0.98 ± 0.04	2.18 ± 0.09 Å
Second sp^3	0.86	0.04 ± 0.04	6.7 ± 0.09 Å [1]

[1] Assuming that this component is assossicated with the defects in the 2nd layer.

Disappearance of the monolayer band upon hydrogenation:

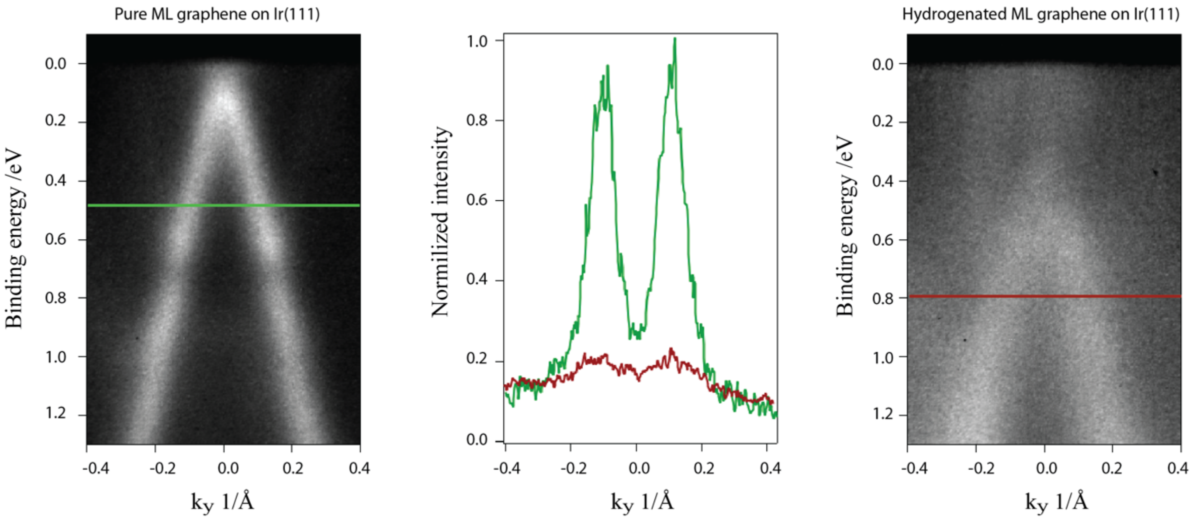

Figure S7: *Comparison of ARPES intensity of the valence band in clean graphene and in hydrogenated graphene on Ir(111) as per reference [7]. The intensities in image data (left and right image) are adjusted in order to show the effect of hydrogenation on the band structure in graphene. The middle graph shows the comparison of intensities when normalized to the maximum intensity in the clean graphene profile. The line profiles shown in the graph are obtained at 0.5eV for clean graphene (green line in the left image) and at 0.8eV in hydrogenated graphene (brown line in the right image).*

In Figure S7 comparison between clean and hydrogenated graphene on Ir(111) is shown. The data are taken from ref. [7]. These data clearly show a strong reduction in the intensity as well as a significant broadening of the valence band upon hydrogenation. These data show the case where the hydrogenation was performed at room temperature using atomic hydrogen while in the present work, hydrogenation is performed by exposure to vibrationally excited molecular hydrogen. However, these two cases are comparable because in both cases only the HCP and FCC parts of graphene/Ir(111) moiré are hydrogenated, *i.e.* at the initial stage of hydrogenation with atomic H and when hydrogenated with excited molecular H_2. See STM images in ref [5] and [7] for comparison. When graphene/Ir(111) is fully hydrogenated with atomic hydrogen, *i.e.* also the ATOP parts of the moiré become hydrogenated, a complete disappearance of the signal from the valence band in graphene takes place.

Table S2: Estimation of the type of doping using the work function difference:

$W_{Ir(111)}$ = 5.7eV

	Work function /eV	**Δc /eV**	**$W_{Ir(111)}$ - W_{gr}- Δc /eV**	**Type of doping**
monolayer	4.5[a]	0.9[a]	0.3	*p*
AB bilayer	4.6[b]	0.5-0.6[c]	0.6-0.5	*p*
ABA trilayer (assuming value close to graphite)	≈4.7	0.56[b]	0.44	*p*
graphite	4.7	-	-	-

Footnotes:
a: Based on [8,9]
b: Based on [10]
c: Based on [11]

The type of doping for graphene in contact with metal is given by:

$$\mathrm{sign}(\Delta E_F) = \mathrm{sign}\,(W_m - W_{gr} - \Delta_c)\ [8,9] \qquad (1)$$

Where positive (negative) value means *p* (*n*) type doping. In equation (1) W_m is the work function of a metal substrate, W_{gr} is the work function of (ML, BL or TL) graphene in free space and Δ_c is a shift due to chemical interaction [8,9] .

References:

[1] Coraux, J., Plasa, T.N., Busse, C. and Michely, T., 2008. Structure of epitaxial graphene on Ir (111). *New Journal of Physics*, *10*(4), p.043033.

[2] Coraux, J., Engler, M., Busse, C., Wall, D., Buckanie, N., Zu Heringdorf, F.J.M., Van Gastel, R., Poelsema, B. and Michely, T., 2009. Growth of graphene on Ir (111). *New Journal of Physics*, *11*(2), p.023006.

[3] Latychevskaia, T., Escher, C. and Fink, H.W., 2019. Moiré structures in twisted bilayer graphene studied by transmission electron microscopy. *Ultramicroscopy*, *197*, pp.46-52.

[4] Presel, F., Tetlow, H., Bignardi, L., Lacovig, P., Tache, C.A., Lizzit, S., Kantorovich, L. and Baraldi, A., 2018. Graphene growth by molecular beam epitaxy: an interplay between desorption, diffusion and intercalation of elemental C species on islands. *Nanoscale*, *10*(16), pp.7396-7406.

[5] Hansen, L.K., 2017. *Tailoring interactions at the graphene-metal interface* (Doctoral dissertation, Aarhus Universitet).

[6] Jørgensen, A.L., Duncan, D.A., Kastorp, C.F., Kyhl, L., Tang, Z., Bruix, A., Andersen, M., Hammer, B., Lee, T.L., Hornekær, L. and Balog, R., 2019. Chemically-resolved determination of hydrogenated graphene–substrate interaction. *Physical Chemistry Chemical Physics*, *21*(25), pp.13462-13466.

[7] Balog, R., Jørgensen, B., Nilsson, L., Andersen, M., Rienks, E., Bianchi, M., Fanetti, M., Lægsgaard, E., Baraldi, A., Lizzit, S. and Sljivancanin, Z., 2010. Bandgap opening in graphene induced by patterned hydrogen adsorption. *Nature materials*, *9*(4), pp.315-319.

[8] Giovannetti, G.A.K.P.A., Khomyakov, P.A., Brocks, G., Karpan, V.V., Van den Brink, J. and Kelly, P.J., 2008. Doping graphene with metal contacts. *Physical review letters*, *101*(2), p.026803.

[9] Khomyakov, P.A., Giovannetti, G., Rusu, P.C., Brocks, G.V., Van den Brink, J. and Kelly, P.J., 2009. First-principles study of the interaction and charge transfer between graphene and metals. *Physical Review B*, *79*(19), p.195425.

[10] Zheng, J., Wang, Y., Wang, L., Quhe, R., Ni, Z., Mei, W.N., Gao, Z., Yu, D., Shi, J. and Lu, J., 2013. Interfacial properties of bilayer and trilayer graphene on metal substrates. *Scientific reports*, *3*, p.2081.

[11] Khan, E., Rahman, T.S. and Subrina, S., 2016. Electronic structure of bilayer graphene physisorbed on metal substrates. *Journal of Applied Physics*, *120*(18), p.185101